Available online at www.sciencedirect.com

SciVerse ScienceDirect

ELSEVIER

Nuclear Physics A 890–891 (2012) 1–10

NUCLEAR PHYSICS A

www.elsevier.com/locate/nuclphysa

Role of Coulomb and nuclear breakups in the interaction of ^{8}B with ^{12}C

B. Paes [a], J. Lubian [a,*], P.R.S. Gomes [a], V. Guimarães [b]

[a] *Instituto de Física, Universidade Federal Fluminense, Av. Litorânea S-N, 24210-340 Niteroi, RJ, Brazil*

[b] *Instituto de Física, Universidade de São Paulo, 05389-970, SP, Brazil*

Received 8 June 2012; received in revised form 19 July 2012; accepted 25 July 2012

Available online 27 July 2012

Abstract

We investigate the breakup of the proton halo ^{8}B projectile in the presence of the light target ^{12}C at near barrier energies. Our calculations show that the effect of the breakup on the elastic scattering angular distributions is negligible. We also investigate the relative importance of Coulomb and nuclear breakups for this system. We compare the results of our calculations with those for the ^{6}He + ^{12}C and ^{8}B + ^{58}Ni systems.

Keywords: Breakup; Elastic scattering

1. Introduction

The effect of the breakup of weakly bound nuclei, both stable and radioactive, on different reaction mechanisms has been a subject of great interest in the last years [1–3]. Different approaches are used in these studies. Particularly interesting cases are the investigations of the role of the breakup on the elastic scattering, and consequently on the total reaction cross section, the effect of the breakup process on the fusion cross section and the magnitude of the breakup itself.

The investigation of the coupling of the elastic channel to breakup states is a difficult task. The reason lies in the fact that the matrix elements of the transition between bound and unbound, or between unbound states, diverge. There are two main methods to overcome this problem within the so-called continuum discretized coupled channel (CDCC) [4,5] method. The first one

* Corresponding author.
E-mail address: lubian@if.uff.br (J. Lubian).

0375-9474/$ – see front matter
http://dx.doi.org/10.1016/j.nuclphysa.2012.07.011

is to expand the whole system wave function into the complete state or pseudo-state basis. Among the most used expansions are the Gaussian [6] and the hyperspherical harmonics expansion [7] basis, mainly used in the four-body CDCC calculations. In fact the hyperspherical method is a convenient way of expressing the wave function of the three-body wave function in the so-called hyperspherical coordinates. The second approach is known as the average or binning method [4,5], in which the basis is obtained by averaging fragment's scattering wave functions in some energy intervals (bins) for each relative angular momentum. The equivalence of the two methods has been proved in the case of the projectile breakup in $d + {}^{58}Ni$ scattering at 80 MeV and those of ${}^{6}Li + {}^{40}Ca$ at 156 MeV [8]. Of course, as in almost all coupled channel calculations, the basis is truncated at one point where a sufficient amount of components has been supposedly included. In order to test this supposition, several convergency test are required.

One important question when one investigates the breakup process of weakly bound nuclei is which is the main interaction producing this breakup: the Coulomb or the nuclear interaction? Or how important is the interference between them? The answer to these questions depends on the structure of the weakly bound nucleus involved in the reaction, on the mass and charge of the other interacting partner and the energy region where the interaction occurs. It has been recently shown that the Coulomb dipole breakup is the main reaction mechanism for the ${}^{6}He + {}^{208}Pb$ [9] system, whereas the quadrupole nuclear breakup is the main reaction mechanism in the ${}^{6}He + {}^{12}C$ system [10], where ${}^{6}He$ is a neutron halo projectile. For the ${}^{8}B + {}^{58}Ni$ system, which involves the proton halo projectile, it has been shown that the interference of Coulomb and nuclear interaction plays a very important role in the reaction mechanism describing the elastic scattering and breakup cross section, as well as the energy distribution of the emitted particles [11]. One might expect that for lighter target, the nuclear breakup of the ${}^{8}B$ projectile could predominate over the Coulomb breakup. Recently, Barioni et al. [12] measured the elastic scattering of ${}^{8}B$ on ${}^{12}C$ at energies well above the Coulomb barrier, and they concluded that the effect of the breakup on the elastic scattering cross section is negligible.

In the present work we investigate the breakup of the proton halo ${}^{8}B$ nucleus in the presence of the target ${}^{12}C$ at near barrier energies. In fact, this is a very interesting energy region to be studied, for which there are no available data so far. We hope that our calculations can be confirmed in the near future by new experiments. We study the effect of the breakup on the elastic scattering angular distributions. We compare the effects on the elastic scattering for this system with the ones for the ${}^{6}He + {}^{12}C$ system. We also investigate the relative importance of Coulomb and nuclear breakups for ${}^{8}B + {}^{12}C$ at near barrier energies, and the effect of continuum–continuum couplings on the breakup angular distributions. We also compare the magnitude of breakup for the ${}^{8}B + {}^{12}C$ and ${}^{58}Ni$ systems at this energy regime. In Section 2 we briefly describe the model space used in the present calculations. In Section 3 we show and discuss the results of the calculations. Finally, in Section 4 we present some conclusions.

2. Model space used in the calculations

In the present work we use the same model space as in Refs. [12–14] for the same system, but at higher energies. In those works it was shown that the CDCC calculations were able to describe the elastic scattering, breakup cross section as well as the energy distributions of the breakup fragments. In all the calculations of the present work the FRESCO code [15] was used.

As ${}^{8}B$ is a proton halo projectile, it can be modeled as ${}^{7}Be + p$ with ground state wave function $1p_{3/2}$ corresponding to the lower single-particle states of the proton relative to the ${}^{7}Be$ core, bound by 0.137 MeV. The remaining projectile's states are in the continuum. To model the continuum states we use the average method [4,5]. The continuum wave functions are represented by square-integrable bin wave functions obtained by averaging the ^{7}Be + p scattering wave functions. The discretization of the continuum was carried out up to the maximum bin energy of $\varepsilon_{\text{max}} = 5.0$ MeV. No excitations of the core were taken into account. The target was also considered to be inert, since no important collective degrees of freedom are expected for this nucleus. To evaluate the coupling matrix elements, the spin of the core was neglected, because the ^{7}Be–p interaction used is diagonal to the spin. To describe the continuum excited states of the ^{7}Be + p system at energies near and below the Coulomb barrier we used R-matrix theory instead the usual S-matrix. At this energy regime, although the higher energy bins are closed states, they can be virtually excited, and R-matrix theory accounts for this effect. Moreover, the solution of the coupled equations within the R-matrix theory is more stable than within S-matrix theory.

Schematically the wave function for the states at the continuum with total angular momentum J and z-projection M can be written as

$$\Psi^{JM}(\mathbf{R},\mathbf{r}) = \sum_i \frac{F_i^J(R)}{R}\,\mathcal{Y}_i^{JM}(\hat{\mathbf{R}},\mathbf{r}). \tag{1}$$

In the previous expression the index i stands for the set of quantum numbers $\{\varepsilon_i l_i j_i, L\}$. In Eq. (1), $\mathbf{r}$ represents the internal coordinates of the projectile, that is, the vector joining the proton and the center of the core, $\mathbf{R}$ is the projectile–target separation vector, $\hat{\mathbf{R}}$ represents its angular degrees of freedom. Using the expansion of Eq. (1), one obtains the coupled channel equations by integrating by all the variables, but R

$$\left[T_L + U_{ii}^J(R) - E + \epsilon_i\right] F_i^J(R) = -\sum_j U_{ij}^J(R) F_j^J(R). \tag{2}$$

The index $i = 0$ stands for the elastic channel, where both the projectile and the target are in their ground states ($\varepsilon_0 = 0$, $l_0 = 1$, $j_0 = 3/2$ and $I_0 = 0$). Channels with $i > 0$ are associated with continuum bins. In Eq. (2), ϵ_i stands for the total excitation energy of channel i, $\epsilon_i = \varepsilon_i + e_i$, with e_i representing the target's excitation energy.

The projectile–target interaction can be split into two parts, according to the expression

$$V(\mathbf{R},\mathbf{r}) = V_{cT}(\mathbf{R},\mathbf{r}) + V_{pT}(\mathbf{R},\mathbf{r}). \tag{3}$$

The first and the second terms at the right hand side of Eq. (3) correspond respectively to the core–target and the proton–target interactions and are the sum of the Coulomb + nuclear interactions. The matrix elements U_{ij}^J in Eq. (2) are given by

$$U_{ij}^J(R) = \int d\hat{\mathbf{R}}\, d^3\mathbf{r}\, \mathcal{Y}_i^{JM*}(\hat{\mathbf{R}},\mathbf{r}) V(\mathbf{R},\mathbf{r})\, \mathcal{Y}_j^{JM}(\hat{\mathbf{R}},\mathbf{r}). \tag{4}$$

To evaluate the above coupling matrix element, the integration was performed up to $r_{\text{bin}} = 55$ fm for $E_{\text{c.m.}} = 3.60$ and 5.52 MeV and $r_{\text{bin}} = 70$ fm for 9.00 MeV. These distances were enough to guarantee the orthogonality between bin wave functions. The convergency was obtained using $R_{\text{max}} = 500$ fm and the relative projectile–target angular momentum $J_{\text{max}} \leqslant 500\hbar$. The bin wave functions for the core–p interactions were calculated for their relative angular momentum $l \leqslant 2\hbar$.

For the core–target and p–target interaction optical potentials, the so-called São Paulo potential (SPP) was used [16,17]. At this energy regime, the SPP can be considered as a double-folding potential for which it was derived a systematic for the nuclear matter densities [16,17]. Its imaginary part is taken equal to the real part multiplied by the 0.78 strength coefficient. For the p–core

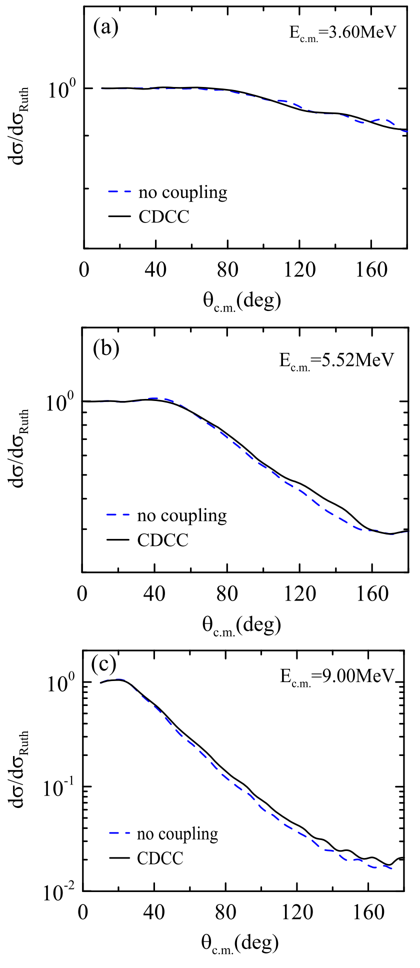

Fig. 1. (Color online.) Comparison of the CDCC results for the elastic scattering angular distributions with the no-coupling results (see the text for details).

interaction, the potential of Ref. [18] was used. The full interaction potential (the sum of the p–target plus core–target Coulomb + nuclear potentials) was expanded in multipoles up to the quadrupole term ($\lambda \leqslant 2$).

3. Results and discussions

3.1. Effect of the breakup on the elastic scattering angular distributions

Fig. 1 shows the results of the CDCC calculations (full curves) for three center-of-mass energies: 3.60 MeV (below the Coulomb barrier), 5.52 MeV (near the barrier) and 9.00 MeV (above the barrier). The results are compared with the calculations for which the couplings were not considered (dashed curves). One can observe that the breakup effect on the elastic scattering angular distribution is rather small, similar to the ones of Ref. [12], obtained for much higher energy. Comparing these results with the ones for the $^{8}B + ^{58}Ni$ system at near barrier energies [13]

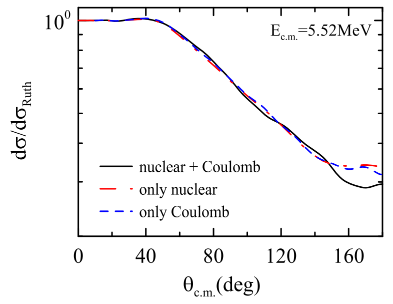

Fig. 2. (Color online.) CDCC results for the elastic scattering angular distributions including only Coulomb and nuclear interactions for the $^8B + ^{12}C$ system (for details, see the text).

(see Fig. 1 of that reference), one concludes that the effect of the breakup of the ^8B proton halo projectile on the elastic scattering decreases with the charge of the target. One might ask whether this is a general property of all halo nuclei. Moreover, is the reason for this small effect the fact that both Coulomb and nuclear breakup are weak or may they be strong, but their interference is strongly destructive? Although these results seem to be evident because the charge of the ^{12}C target is smaller than for the ^{58}Ni, there are contradictory experimental results in the literature concerning the effect of the breakup on fusion and total reaction cross sections as a function of the charge of the target [19–24]. In these references it is shown that the complete fusion suppression and total reaction cross sections above the barrier energy for weakly bound systems depend on the charge of the target, whereas the total fusion cross section (sum of complete fusion plus the incomplete fusion of part of the projectile) is not affected by the breakup at the same energy range for any target mass (or charge).

In order to study the relative importance of the Coulomb and nuclear breakups, we switch on and off the Coulomb (nuclear) part of the interaction potentials (3) in the transition matrix elements (4). In Fig. 2 we show the results for the Coulomb (dashed curve) and nuclear (dot-dashed curve) breakups for the elastic angular distribution at 5.52 MeV. One can observe that the effects of both nuclear and Coulomb breakups are also very small.

In Fig. 3 we compare the breakup effect on the elastic scattering angular distribution of the present system with the one for the $^6He + ^{12}C$ system. In order to compare results for different systems, we follow the prescription of Refs. [20–22,24]. In those references it is shown that the same physical conditions for different systems are present when the dimensionless quantity $x = (E_{c.m.} - V_B)/\hbar\omega$ is the same for them, where $\hbar\omega$ is the curvature of the barrier in the parabolic model. In Ref. [10], the authors performed four-body CDCC calculations that agree very well with the experimental data for incident ^6He neutron halo radioactive beam with $E_{c.m.} =$ 18 MeV, corresponding to $x = 6.34$ ($V_B = 1.96$ MeV, $\hbar\omega = 1.82$ MeV). For the $^8B + ^{12}C$ system ($V_B = 5.14$ MeV, $\hbar\omega = 2.72$ MeV), the same value of x is obtained for $E_{c.m.} = 22.38$ MeV, according to the SPP predictions. The CDCC results for both systems (full curves) for this value of x and the results for no-coupling calculations (dashed curves) are shown in Fig. 3. One can observe that the effect of the breakup on the elastic scattering is much more important for the system involving the neutron halo projectile ^6He than the proton halo ^8B. It would be interesting to investigate whether this behavior is a characteristic of the ^8B projectile or if it is a general property of other proton halo projectiles. For this reason, further investigations on this line are required to support this conclusion. So far it is not possible to extend the above conclusion for

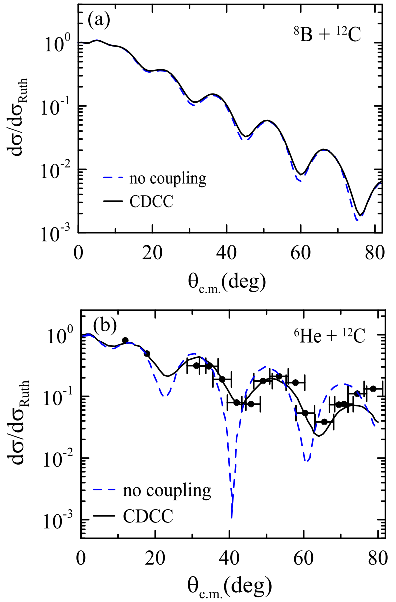

Fig. 3. (Color online.) Comparison of the CDCC results for the elastic scattering angular distributions with the no-coupling results for the $^{8}B + {}^{12}C$ system (a) and $^{6}He + {}^{12}C$ system (b) at $x = 6.34$. The experimental data for the $^{6}He + {}^{12}C$ system were taken from Ref. [25] (for details, see the text).

systems with heavy targets because there are no calculations with different targets available at the same *physical conditions* (same value of x).

3.2. Breakup angular distributions

In this section we investigate the relative importance of Coulomb and nuclear breakup by studying their angular distributions. The results of the CDCC calculations are shown in Fig. 4. The full curves represent the CDCC calculations including the Coulomb plus nuclear interactions. The dashed curves represent the calculations where the Coulomb interaction has been switched off, while the dot-dashed curves correspond to the situation where the Coulomb interaction was switched off. We would like to stress that in these calculations there is one important difference when compared to the calculations of Fig. 2. In the Fresco code, when one switches off the nuclear interaction, the code automatically takes away the nuclear part of the optical potential used to describe the elastic scattering. To compare the various options of Fig. 2 we have kept the diagonal nuclear optical potential of the ground state channel. In order to compare our results to the ones of Ref. [14], we eliminated the diagonal part of the nuclear optical potential when calculating the breakup cross sections with only Coulomb interactions, i.e., all the nuclear interactions were completely eliminated. From Fig. 4 one observes that the Coulomb and nuclear breakups interfere destructively, in agreement with the conclusions of Ref. [14], obtained for the ^{58}Ni target. From Table 1, where are shown the integrated cross sections for the angular distributions shown in Fig. 4, it is possible to notice that the nuclear breakup is more important than the Coulomb breakup for this system at near barrier energies. At energies below Coulomb barrier, this is clearly observed in the whole angle interval (Fig. 4a). At energies above barrier, the nuclear breakup is more important at forward angles (Fig. 4c). It has been recently shown by means

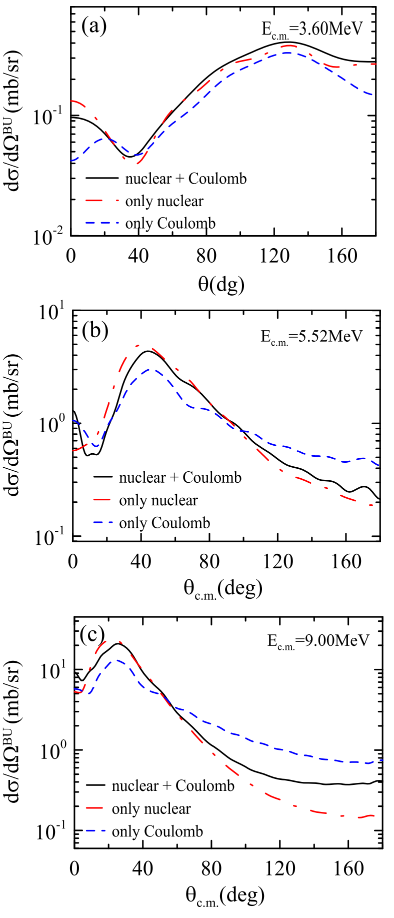

Fig. 4. (Color online.) Relative importance of the Coulomb and nuclear couplings on the breakup angular distributions (for details, see the text).

of measurement of experimental breakup cross section at energies well above the Coulomb barrier, that the nuclear breakup cross section of systems involving ^{8}B projectile is bigger than the Coulomb breakup [26–29]. Naively, one could expect that the reactions involving the proton halo projectile might be dominated by Coulomb breakup. But in some cases quantum mechanic calculations show the opposite. Recently, it has been shown that the use of effective parameters, such as effective binding energies, makes the proton behave similar to neutron [30,31]. By using these effective binding energies the net effect that is obtained for the proton–target interaction is to lower the Coulomb barrier of its interaction. So, according to these theoretical works, the reason for the nuclear breakup being bigger than the Coulomb breakup for proton halo projectile is the Coulomb repulsion between the proton and the target. On the other hand, other authors have obtained exactly the opposite results, i.e., that the Coulomb breakup is the dominant reaction mechanism in the dissociation of the ^{8}B projectile by studying its interaction with heavy targets at high energies [32,33]. Their calculations agree well with recent experimental data [34,35] obtained from the ^{8}B breakup on lead targets. A good description of the experimental *S*-factors of astrophysical interest at low energies was also obtained by considering that the main breakup

Table 1
Integrated breakup cross sections (in mb) for different CDCC calculations.

$E_{c.m.}$ (MeV)	Only coul.	Only nucl.	Coul. + nucl.
3.60	2.31	2.69	2.95
5.52	15.24	20.20	18.41
9.00	36.17	39.99	39.72

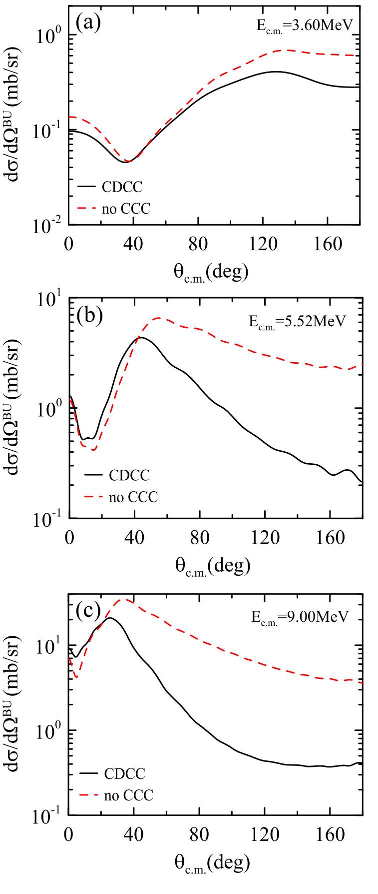

Fig. 5. (Color online.) Effect of continuum–continuum couplings on the breakup angular distributions (see the text for details).

mechanism (the way of obtaining the radioactive capture cross section by inverse kinematics) is the Coulomb one [33,36], in agreement with experimental data reported in the literature. On the light of these contradictions, it would be very important to perform theoretical calculations on the same footing covering large energy and target mass ranges of reactions involving the ^{8}B projectile.

In Fig. 5 we show the effect of the continuum–continuum couplings (CCCs) on the breakup angular distributions for the same three energies. The solid curves represent the full CDCC calculations, where CCCs are included, and the dashed curves are results of the calculations when

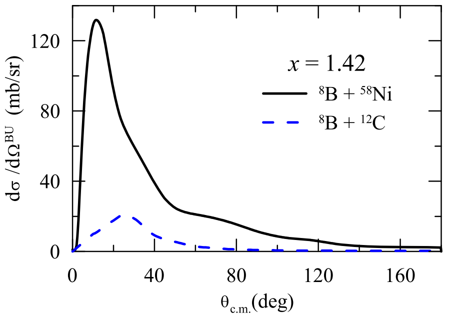

Fig. 6. (Color online.) Comparison of the breakup angular distributions of the ^{8}B + ^{12}C and ^{8}B + ^{58}Ni systems at $x = 1.42$ (see the text for details).

the CCCs are switched off. One can observe that the CCCs play a very important role on the breakup cross sections for the ^{8}B + ^{12}C system and its effect is to lower the breakup cross section, as predicted for the ^{8}B +^{58} Ni system [37]. The effect of CCCs on the elastic scattering angular distributions was found to be negligible (not shown).

In Fig. 6 we compare the breakup angular distributions for the ^{8}B+^{12} C and ^{8}B+^{58}Ni systems at the same physical conditions ($x = 1.42$). The choice of this value of the dimensionless variable x corresponds to the existence of theoretical calculations for breakup in the ^{8}B + ^{58}Ni system at the same value [38]. The full curve corresponds to the ^{58}Ni target, while the dashed curve corresponds to the ^{12}C target. One can observe that the breakup cross section for the heavier target is much larger than for the lighter. In Ref. [23], it has been shown that the breakup effect on the reaction cross section for the ^{8}B + ^{58}Ni system is remarkable (for more details see Fig. 2 of Ref. [23]), whereas in Ref. [12] it has been shown that for the ^{8}B + ^{12}C system, at energies well above Coulomb barrier, it is negligible. From the present results, one can expect that at near barrier energies the effect of breakup would be also very weak for this system. This conclusion comes from the fact that the breakup does not affect the elastic cross section (see Fig. 1), and that the breakup cross section is very small (see Fig. 6).

4. Summary and conclusions

We have shown that the effect of Coulomb and nuclear breakup of the proton halo ^{8}B in the elastic scattering by the light target ^{12}C is negligible at near barrier energies, similar to what has been previously verified at higher energies. Since this effect is not negligible in the elastic scattering of ^{8}B by the heavier ^{58}Ni target, one might conclude that this is due to the very small charge and mass of this light system. However, for the scattering of ^{6}He on ^{12}C, the breakup effect is important at higher energies. We can thus conclude that the breakup of the proton halo ^{8}B is significantly different from the breakup of the neutron halo ^{6}He. The total reaction cross section should not be increased in the presence of the ^{8}B breakup in the neighboring of a light target. It would be interesting to investigate whether the same holds for the elastic scattering cross section of neutron rich isotope projectiles as ^{12}B and ^{13}B on ^{12}C and ^{58}Ni targets. Such measurements are being planned. Also, the comparison of ^{8}B and ^{13}B elastic scattering and/or breakup measurements on some other targets, such as ^{120}Sn would be interesting to investigate the charge dependence on these mechanisms.

We also investigate the relative importance of Coulomb and nuclear breakups for this system. The nuclear breakup is shown to be slightly more important than the Coulomb breakup at near barrier energies. We show that the continuum–continuum couplings play a very important role in the breakup cross section. Finally we show that the breakup cross section for the $^{8}B + ^{12}C$ system is much smaller than for $^{8}B + ^{58}Ni$.

Acknowledgements

The authors would like to thank CNPq, FAPERJ, CAPES and the Pronex for their partial financial support.

References

[1] L.F. Canto, P.R.S. Gomes, R. Donangelo, M.S. Hussein, Phys. Rep. 424 (2006) 1.
[2] J.F. Liang, C. Signorini, Intern. J. Mod. Phys. E 14 (2005) 1121.
[3] N. Keeley, R. Raabe, N. Alamanos, J.L. Sid, Prog. Part. Nucl. Sci. 59 (2007) 579.
[4] M. Kamimura, et al., Prog. Theor. Phys. Suppl. 89 (1986) 1.
[5] N. Austern, et al., Phys. Rep. 154 (1987) 125.
[6] E. Hiyama, et al., Prog. Part. Nucl. Phys. 51 (2003) 223.
[7] M. Rodriguez-Gallardo, et al., Phys. Rev. C 77 (2008) 064609.
[8] T. Matsumoto, et al., Phys. Rev. C 68 (2003) 064607.
[9] K. Rusek, et al., Phys. Rev. C 72 (2005) 037603.
[10] T. Matsumoto, et al., Phys. Rev. C 70 (2004) 061601(R).
[11] F.M. Nunes, I.J. Thompson, Phys. Rev. C 57 (1998) R2818.
[12] A. Barioni, et al., Phys. Rev. C 84 (2011) 014603.
[13] J. Lubian, et al., Phys. Rev. C 79 (2009) 064605.
[14] J.A. Tostevin, F. Nunes, I. Thompson, Phys. Rev. C 63 (2001) 024617.
[15] I.J. Thompson, Comput. Phys. Rep. 7 (1988) 167.
[16] L.C. Chamon, et al., Phys. Rev. Lett. 79 (1997) 5218.
[17] L.C. Chamon, et al., Phys. Rev. C 66 (2002) 014610.
[18] H. Esbensen, G.F. Bertch, Nucl. Phys. A 60 (1996) 37.
[19] P.R.S. Gomes, et al., Phys. Rev. C 84 (2011) 014615.
[20] L.F. Canto, et al., J. Phys. G 36 (2009) 015109.
[21] L.F. Canto, et al., Nucl. Phys. A 821 (2009) 51.
[22] P.R.S. Gomes, L.F. Canto, J. Lubian, M.S. Hussein, Phys. Lett. B 695 (2011) 320.
[23] J.M.B. Shorto, et al., Phys. Rev. C 81 (2010) 044601.
[24] P.R.S. Gomes, J. Lubian, L.F. Canto, Phys. Rev. C 79 (2009) 027606.
[25] M. Milin, et al., Nucl. Phys. A 730 (2004) 285.
[26] B. Blank, et al., Nucl. Phys. A 624 (1997) 242.
[27] D. Cortina-Gil, et al., Nucl. Phys. A 720 (2003) 2.
[28] C. Borcea, et al., Nucl. Phys. A 616 (1997) 231c.
[29] F. Negoita, et al., Phys. Rev. C 54 (1996) 1787.
[30] A. Bonaccorso, D.M. Brink, C.A. Bertulani, Phys. Rev. C 69 (2004) 024615.
[31] R. Kumar, A. Bonaccorso, Phys. Rev. C 84 (2011) 014613.
[32] C.A. Bertulani, M. Gai, Nucl. Phys. A 636 (1998) 227.
[33] C.A. Bertulani, Z. Phys. A 356 (1996) 293.
[34] T. Motobayashi, et al., Phys. Rev. Lett. 73 (1994) 2680.
[35] T. Kikushi, et al., Phys. Lett. B 391 (1997) 261.
[36] P. Navratil, C.A. Bertulani, E. Caurier, Nucl. Phys. A 787 (2007) 539c.
[37] L.F. Canto, J. Lubian, P.R.S. Gomes, M.S. Hussein, Phys. Rev. C 80 (2009) 047601.
[38] J. Lubian, F.M. Nunes, J. Phys. G 34 (2007) 513.